

# Status Report on Fast Flux Test Facility Mechanistic Fuel Failure Experiment Analysis with BISON for Post Irradiation Examination Support

May 2024

*Revision 0*

Alexander Swearingen, Kyle Paaren, Pavel Medvedev  
Idaho National Laboratory





#### **DISCLAIMER**

This information was prepared as an account of work sponsored by an agency of the U.S. Government. Neither the U.S. Government nor any agency thereof, nor any of their employees, makes any warranty, expressed or implied, or assumes any legal liability or responsibility for the accuracy, completeness, or usefulness, of any information, apparatus, product, or process disclosed, or represents that its use would not infringe privately owned rights. References herein to any specific commercial product, process, or service by trade name, trade mark, manufacturer, or otherwise, does not necessarily constitute or imply its endorsement, recommendation, or favoring by the U.S. Government or any agency thereof. The views and opinions of authors expressed herein do not necessarily state or reflect those of the U.S. Government or any agency thereof.





# **Status report on Fast Flux Test Facility Mechanistic Fuel Failure Experiment Analysis with BISON for Post Irradiation Examination Support**

***Revision 0***

Alexander Swearingen, Kyle Paaren, Pavel Medvedev

**May 2024**

**Idaho National Laboratory  
Idaho Falls, Idaho 83415**

**<http://www.inl.gov>**

**Prepared for the  
U.S. Department of Energy  
Office of Nuclear Energy  
Under DOE Idaho Operations Office  
Contract DE-AC07-05ID14517**





*Page intentionally left blank*





### ABSTRACT

The renewed interest in metallic U-Zr nuclear fuel alloy has led to a drive for deeper understanding of the mechanisms driving the phenomena observed under irradiation conditions. The Department of Energy Advanced Fuel Campaign has developed infrastructure to support metallic fuel development, including Post Irradiation Examination (PIE) of legacy Fast Flux Test Facility (FFTF) Mechanistic Fuel Failure (MFF) experiments. The PIE performed on legacy FFTF MFF experiments gives insight on metallic fuel performance and can address the lack of knowledge and scarcity of reliable data identified in several studies over recent years. Unfortunately, PIE efforts can cost significant time and resources which can impede the progress of metallic U-Zr fuel development. Metallic U-Zr fuel performance modeling can be used to inform PIE efforts on regions of interest for relevant investigations and can help understand phenomena observed in PIE. This report demonstrates the current progress of FFTF MFF fuel performance simulations using the BISON fuel performance code and discusses the support provided by simulation to PIE efforts. Progress in temperature, profilometry, fission gas release, plenum pressure, fuel cladding chemical interaction, and zirconium redistribution simulation results have been demonstrated.



*Page intentionally left blank*



## CONTENTS

ABSTRACT .....	iii
ACRONYMS.....	viii
Status report on FFTF MFF Experiment Analysis with BISON for PIE Support.....	1
1. Introduction.....	1
2. FFTF and Metallic fuel experiments.....	1
3. BISON MFF Pin Modelling Methodology .....	4
4. Simulation Results and Comparison with PIE.....	7
4.1 Temperature .....	7
4.2 Profilometry .....	8
4.3 Fission Gas Release and Plenum Pressure.....	9
4.4 Fuel Cladding Chemical Interaction .....	9
4.5 Zirconium Redistribution.....	10
5. Conclusions.....	11
6. References.....	12



## FIGURES

Figure 1. FFTF Series III.b driver fuel assembly [10].....	2
Figure 2. FFTF metallic fuel pin design [10]. ....	2
Figure 3. Coupling of BISON Material Property Models .....	6
Figure 4: Simulated FCT, ICT, and End of Life Burnup for a) 193045 and b) 195011 .....	7
Figure 5: Simulated PFCT and PICT over time for a) 193045 and b) 195011 .....	8
Figure 6: Simulated and Experimental Profilometry Results for a) 193045 and b) 195011 .....	8
Figure 7: Simulated Fractional Zirconium Concentration Compared to Metallography of 193045 [11] .....	11

## TABLES

Table 1. MFF-2, -3, -5 and -6 fuel pin design characteristics, taken from [11]. ....	3
Table 2: FFTF MFF-3 Power, Flux, and Flowrates [8, 12].....	4
Table 3: FFTF MFF-5 Power, Flux, and Flowrates [8, 12].....	5
Table 4. BISON Material Model Objects .....	5
Table 5: Burnup, Plenum Pressure, and Fission Gas Released Comparison [11] .....	9
Table 6: Comparison of Simulated FCCI with PIE [11] .....	10





*Page intentionally left blank*



## ACRONYMS

AFC	Advanced Fuels Campaign
DOE	Department of Energy
EBR-II	Experimental Breeder Reactor II
FCCI	Fuel Cladding Chemical Interaction
FCMI	Fuel Cladding Mechanical Interaction
FCT	Fuel Centerline Temperature
FFTF	Fast Flux Test Facility
HFEF	Hot Fuel Examination
ICT	Inner Cladding Temperature
INL	Idaho National Laboratory
MFC	Materials and Fuels Complex
MFF	Mechanistic Fuel Failure
PFCT	Peak Fuel Centerline Temperature
PICT	Peak Inner Cladding Temperature
PIE	Post Irradiation Examination
SFR	Sodium Fast Reactor



*Page intentionally left blank*



## Status report on FFTF MFF Experiment Analysis with BISON for PIE Support

### 1. Introduction

The metallic U-Zr nuclear fuel alloy has resurfaced as one of the most promising fuel candidates for next generation sodium-cooled fast reactors (SFRs). Some advantages of the fuel form include higher densities of fissile and fertile material loading compared to most other fuel systems, providing excellent reactor core performance both in normal and off-normal conditions, and relatively high thermal conductivities [1-3]. Also, fabrication of the U-Zr fuel form is relatively simple and has the capability of being recycled with proven technology such as melt refining or electro-refining processes [4].

Historically, U-Zr fuel has been investigated several times for use in reactors. Experimental Breeder Reactor II (EBR-II) Mark III/IIIA/IV driver fuel (U-10Zr fuel with austenitic stainless steel (CW316 or CWD9), and ferritic martensitic steel HT-9 cladding) was irradiated up to at least 10at.%. There were also several experimental assemblies in both EBR-II and the Fast Flux Test Facility (FFTF) in which fuel pins achieved higher peak burnup, and demonstrated safe operation without failure [2]. In recent years multiple studies such as gap assessment reports [5], fuel design basis reports [6] and research needs reports [7] have pointed out several areas in which improvement, lack of knowledge, and scarcity of reliable data need to be addressed to allow a U-Zr fuel design basis to be qualified for commercial use.

The Department of Energy Advanced Fuel Campaign (DOE AFC) has performed research and development activities to implement infrastructure in support of metallic fuel technology maturation. Within this mandate and renewed interested in metallic fuel, AFC has laid out a 5-year R&D plan for metallic fuel (to be published) in which a thorough review of the different fuel performance phenomena is provided, the existing gaps are acknowledged and a workplan is described to reduce uncertainties for potential customers (e.g. industries, NRC, international partners) to be able to bring metallic fuel technology to commercialization.

This report on simulations of the FFTF Mechanistic Fuel Failure (MFF) experiments performed in the BISON fuel performance code for support of Post Irradiation Examination (PIE) will address key gaps identified by the AFC 5-year R&D plan. Specifically, this report will demonstrate the current capabilities of the BISON fuel performance code to simulate FFTF MFF experiments and the ability of using simulations to inform PIE efforts. This report is divided into several sections. Section 2 briefly describes the irradiation testing and fuel design characteristics of the FFTF MFF experiments. In Section 3 the modelling methodology is discussed. This includes rationale for any assumptions made. Section 4 presents detailed simulation results for several pins and a comparison between simulation results and PIE exam results. Finally, Section 5 presents some preliminary conclusions.

### 2. FFTF and Metallic fuel experiments

The FFTF, operated from 1982 to 1992, is the latest SFR to be designed, constructed, and operated by the U.S. DOE with the mission to aid in testing advanced fuels and materials for U.S. SFR research [8, 9]. Driver fuel was U, Pu mixed oxide (MOX) and fuels tested within the FFTF included  $\text{UO}_2$  and mixed-oxide fuels with burnups as high as 16 at.% and linear heat generation rates (LHGRs) exceeding  $60 \text{ kW}\cdot\text{m}^{-1}$  [10]. Metallic U-10Zr fuel was also tested to be qualified as driver fuel through a test campaign of various metallic fuel assemblies. The aim of this test campaign was to answer some remaining questions about long



length metallic fuel pin and assembly designs (e.g. possible length/weight or aspect ratio effect) compared to the EBR-II design.

The MFF test assemblies irradiated in FFTF are denoted MFF-1 and -1A (lead metal fuel test), MFF-2 and -3 (metal prototype) and MFF-5 and -6 (Series III.b qualification) for a total of 1050 U-10Zr fuel pins irradiated. Figure 1 and Figure 2 report the schematic of Series III.b driver fuel assembly and metallic fuel pin design, respectively.

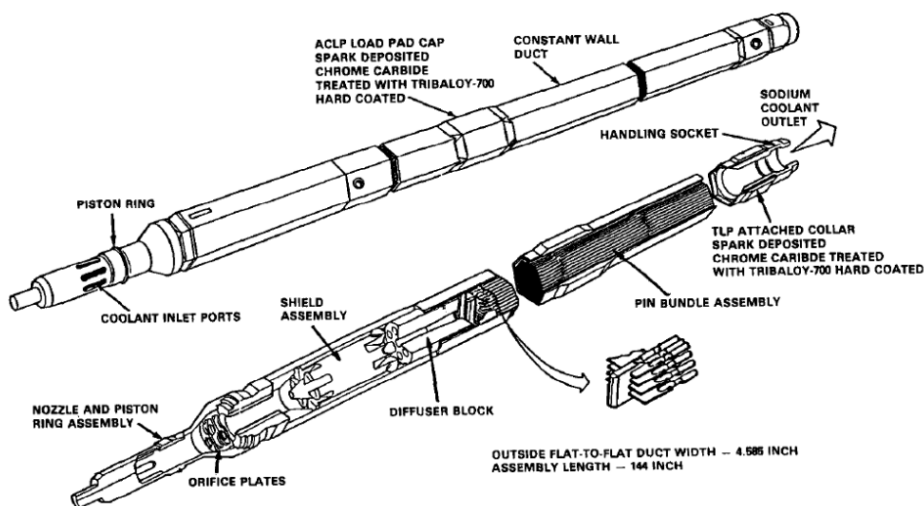


Figure 1. FFTF Series III.b driver fuel assembly [10].

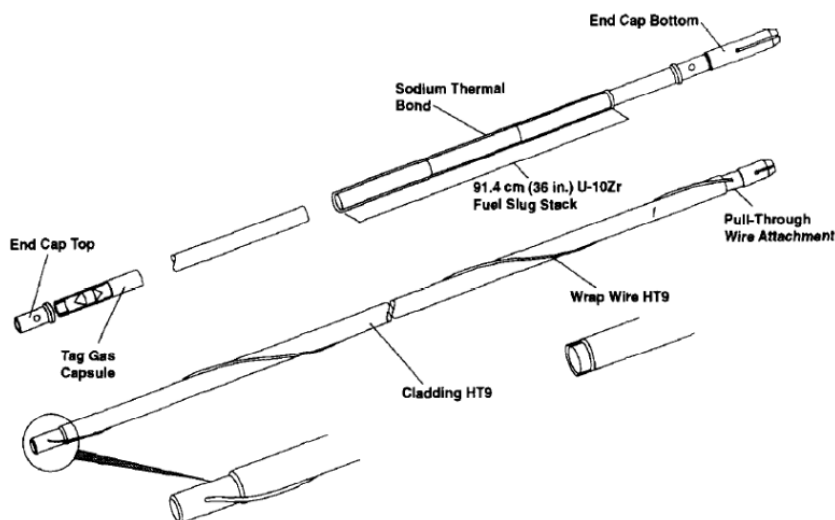


Figure 2. FFTF metallic fuel pin design [10].

To address the scope discussed in the introduction, only the prototype and Series III.b assemblies are considered for this work. The MFF-2, MFF-3, MFF-5, and MFF-6 assemblies each contained 169 binary U-10Zr fuel pins and used HT-9 cladding. Like the design of EBR-II fuel pins, MFF assemblies used a sodium bond between the fuel and the cladding for increased heat transfer, allowing for higher LHGRs.



Fast neutron fluence values observed within the MFFs were similar to EBR-II high-burnup experiments, with values reaching  $2 \times 10^{23} \text{ n}\cdot\text{cm}^{-2}$ . These high ( $E > 0.1 \text{ MeV}$ ) fast neutron fluence values allow for irradiation effects to occur, such as FCCI. Table 1 reports the fuel pin design characteristics.

Table 1. MFF-2, -3, -5 and -6 fuel pin design characteristics, taken from [11].

	MFF-2&3	MFF-5&6
Fuel Slug		
diameter (mm)	4.98	4.98
length (cm)	91.4	91.4
composition	U-10Zr	U-10Zr
density ( $\text{g}/\text{cm}^3$ )	15.8	15.8
mass slug (g)	281.3	281.3
wt% U	90	90
mass U (g)	253.2	253.2
$^{235}\text{U}$ enrichment (%)	32.4	31.0
mass $^{235}\text{U}$ (g)	82.05	78.5
mass $^{238}\text{U}$ (g)	171.1	174.7
wt% Zr	10	10
mass Zr (g)	28.1	28.1
Axial Reflector		
material	Inconel	Inconel
number	1	1
diameter (mm)	4.81	4.81
length (cm)	16.5	6.4
Cladding		
OD (mm)	6.86	6.86
thickness (mm)	0.559	0.559
Wire wrap diameter/pitch (mm/cm)	1.35/15.24	1.35/22.86
material	HT-9	HT-9
Other Characteristics		
sodium fill above fuel (cm)	2.54	2.54
total Pin Length (cm)	238	237
smeared density, %	75.2	75.2
gas plenum volume ( $\text{cm}^3$ @ 25°C)	28.9	31.5



### 3. BISON MFF Pin Modelling Methodology

The BISON fuel performance code has been used to simulate the thermomechanical behaviors of the MFF experiments described in section 2. These simulations are dependent on information on the irradiation conditions of the experiment. Irradiation conditions for the MFF series pins were archived through Pacific Northwest National Laboratory (PNNL). Within the PNNL reports, MFF-2, MFF-3, MFF-5 and MFF-6 assembly power, flux, and flowrates are given at the beginning (BOC) and end (EOC) of each power cycle, with the exception of Cycles 10C-2, 11A-1, and 11A-2. These three cycles did not contain any EOC data due to their short duration [12]. In addition, assembly axial power and flux profiles are supplied at the BOC and EOC with the same exceptions. As an example, FFTF MFF-3 and MFF-5 power, flux, and flowrate values for each power cycle are listed in Tables 2 and 3. The average assembly powers were divided by the number of pins in each assembly (169) and the fuel pin length to generate a homogeneous linear heat generation rate (LHGR) for each fuel pin at each power cycle for each MFF assembly. To obtain the unique power profile and LHGR for each pin, the assembly-average LHGR and flux values were then multiplied by their respective assembly power distribution and axial power and flux profiles for each power cycle. Since power and flux are functions of axial height (location) and time, bilinear functions are used within BISON to describe pin conditions [13].

Table 2: FFTF MFF-3 Power, Flux, and Flowrates [8, 12]

Power Cycle	Fission Power (MW)	Fast Flux ( $\text{n}\cdot\text{cm}^{-2}\cdot\text{s}^{-1}$ )	Flowrate ( $\text{lb}\cdot\text{hr}^{-1}$ )
B10C-1	7.94	2.50E+15	203000
E10C-1	7.72	2.48E+15	203000
B/E10C-2	7.73	2.48E+15	203000
B10C-3	7.70	2.47E+15	203000
E10C-3	7.53	2.46E+15	203000
B/E11A-1	7.39	2.48E+15	202240
B/E11A-2	7.41	2.48E+15	202240
B11A-3	7.27	2.44E+15	202240
E11A-3	7.00	2.43E+15	202240
B11B-1	7.01	2.47E+15	204240
E11B-1	6.77	2.45E+15	204240
B11B-2	6.64	2.42E+15	197960
E11B-2	6.31	2.39E+15	197960
B11C	6.27	2.25E+15	197790
E11C	6.13	2.41E+15	197790
B12A-1	5.89	2.31E+15	193950
E12A-1	5.80	2.31E+15	193950
B12A-2	5.76	2.30E+15	193800
E12A-2	5.68	2.30E+15	193800
B12B-1	5.91	2.43E+15	195840
E12B-1	5.81	2.42E+15	195840
B12B-2	5.71	2.39E+15	195840
E12B-2	5.62	2.39E+15	195840



Table 3: FFTF MFF-5 Power, Flux, and Flowrates [8, 12]

Power Cycle	Fission Power (MW)	Flux ( $\text{n}\cdot\text{cm}^{-2}\cdot\text{s}^{-1}$ )	Flowrate ( $\text{lb}\cdot\text{hr}^{-1}$ )
B11B-1	7.55	2.40E+15	200400
E11B-1	7.29	2.39E+15	200400
B11B-2	7.47	2.60E+15	194240
E11B-2	7.02	2.56E+15	194240
B11C	6.98	2.62E+15	194070
E11C	6.79	2.57E+15	194070
B12A-1	7.13	2.78E+15	190310
E12A-1	6.93	2.75E+15	190310
B12A-2	6.98	2.78E+15	190160
E12A-2	6.79	2.75E+15	190160
B12B-1	6.87	2.80E+15	192170
E12B-1	6.68	2.77E+15	192170
B12B-2	6.70	2.79E+15	192170
E12B-2	6.52	2.76E+15	192170

Table 4. BISON Material Model Objects

Phenomenon	Fuel Model	Cladding Model
Fuel Phase	PhaseUPuZr [13]	N/A
Thermal Conductivity	ThermalUPuZr [14, 15]	ThermalHT9 [16]
Density ( $\text{g}\cdot\text{cm}^{-3}$ )	15.8	7.8
Burnup	UPuZrBurnup [17]	N/A
Fission Rate	UPuZrFissionRate [18]	N/A
Elasticity Tensor	UPuZrElasticityTensor [16]	HT9ElasticityTensor [19]
Creep	UPuZrCreepUpdate [16]	HT9CreepUpdate [16]
Thermal Expansion	UPuZrThermalExpansionEigenstrain [20]	HT9ThermalExpansionEigenstrain [21]
Gaseous Swelling with Hot-pressing pore collapse	ADSimpleFissionGasViscoplasticityStressUpdate [17, 22, 23] ADUPuZrHotPressingStressUpdate [17, 22, 23] PorosityfromStrain [18]	N/A
Fission Gas Release	ADSimpleFissionGasViscoplasticityStressUpdate [17, 22, 23]	N/A
Solid Swelling	BurnupDependentEigenstrain [22]	N/A
Cladding Void Swelling	N/A	HT9VolumetricSwellingEigenstrain [16]
FCCI	N/A	MetallicFuelWastage [18] MetallicFuelWastageDamage [18]
CDF	N/A	FailureCladHT9 [24]





The unique LHGR, cladding temperatures, and fast neutron fluence experienced by the MFF experiments produced a plethora of different fuel performance behaviors. These behaviors include cladding creep (thermal and irradiation-induced), irradiation-induced void swelling, fuel cladding mechanical interaction (FCMI) and fuel cladding chemical interactions (FCCI). MFF-3 and -5 experiments had higher cladding temperatures compared to MFF-2 and -6, which ran colder. The hotter pins experienced more thermal creep and FCCI, which created strain in the cladding near the top of the fuel column. Higher burnup pins such as the pin in the MFF-2 and -3 experiments allowed for more FCMI and created more cladding strain near the fuel axial centerline, and more fission products within the fuel-cladding interface. The BISON fuel performance code has been used to simulate these behaviors for each MFF pin. Geometric information, initial and boundary conditions, and power and flux histories from each pin were supplied from the PNNL reports to be used in conjunction with material models and contact actions within BISON. The simulations utilize mortar formulation mechanical and thermal contact between the fuel and cladding to simulate FCMI and heat transfer through the sodium bond. Material properties for both the fuel and cladding are simulated by using the models found in Table 4. The MFF pins are U-Zr metallic fuel instead of the U-Pu-Zr metallic fuel that are referenced in the models. These models are still applicable to U-Zr fuel if the initial Pu content is provided as zero. The interconnection of the material models used in the MFF simulations is shown in Figure 3.

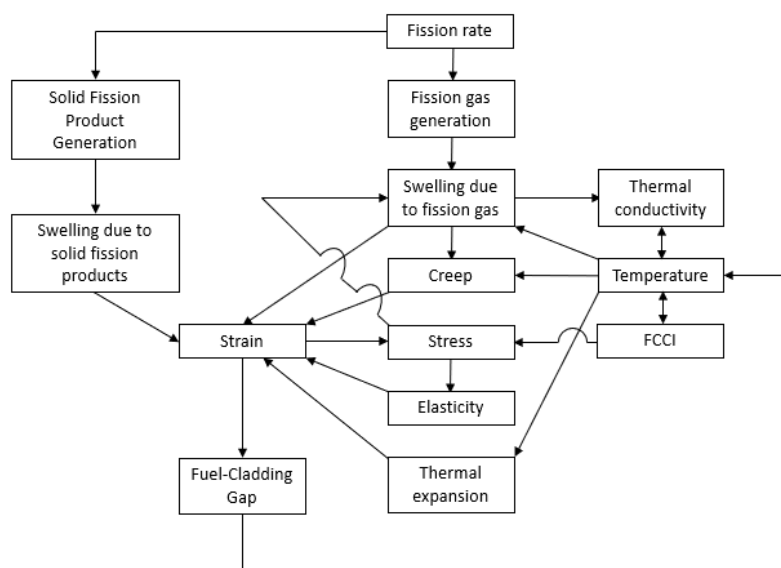


Figure 3. Coupling of BISON Material Property Models

These simulations were performed to support qualification and validation efforts of metallic fuel, in addition to providing insight into the material properties over each irradiation. These material properties include fuel and cladding temperature histories, zirconium redistribution predictions, and FCCI degradation. Peak centerline fuel temperature (PCFT), peak inner clad temperature (PICT), average inner cladding temperature, average fuel centerline temperature, and axial fuel burnup were also predicted over each irradiation history. The simulation of these average predicted temperature profiles and material property evolution over time allow for informed PIE selection, such as cut locations for destructive testing.



## 4. Simulation Results and Comparison with PIE

The MFF BISON simulations offer insight into the possible fuel performance behaviors via models developed from previously observed outcomes. This allows for guided selection of PIE locations as we can use the simulation predictions to determine likely high-value sections of experiments to evaluate. The following sections will demonstrate the current simulation results and discuss the ways that this information might inform PIE investigations. Also, where available, the simulations will be compared with currently available PIE results. This comparison will help in establishing current error within the simulation results and margins when applying these results to PIE selection. Specifically, the results discussed will include fuel and cladding temperatures, profilometry, fission gas release, plenum pressure, FCCI, and zirconium redistribution for the selected MFF pins.

### 4.1 Temperature

Temperature is a significant driver of many fuel performance metrics within the fuel and cladding such as creep and FCCI. By having a sufficient understanding of the temperature evolution throughout the life of the MFF pins, regions of interest can be prioritized for investigation with PIE. Comparisons of the temperature to axial position are useful for determining the regions of interest. Fuel Centerline Temperature (FCT) and Inner Cladding Temperature (ICT) has been simulated for each of the 169 pins. Figure 4 shows the FCT and ICT as a function of axial position for a single representative pin from each experiment. Figure ## also includes the burnup at the end of life for each pin shown. These plots demonstrate that the FCT is lower axially than the ICT and that the highest burnup is lower than both. This informs researchers on which sections will have conditions relevant to the phenomena they are interested in studying and allows them to target the best sections for investigation.

Furthermore, the evolution of the temperature over time can be simulated at specific axial points to investigate the temperature experienced by selected sections. Figure 5 shows the PFCT and PICT over time for the x/L axial location of 0.45. Each of the pins shown in Figure 4 are also represented in Figure 5. This analysis can inform researchers about approximate constituent redistribution information within the selected section. This information could also inform researchers of any unique temperature scenarios that could lead to unexpected profilometry results.

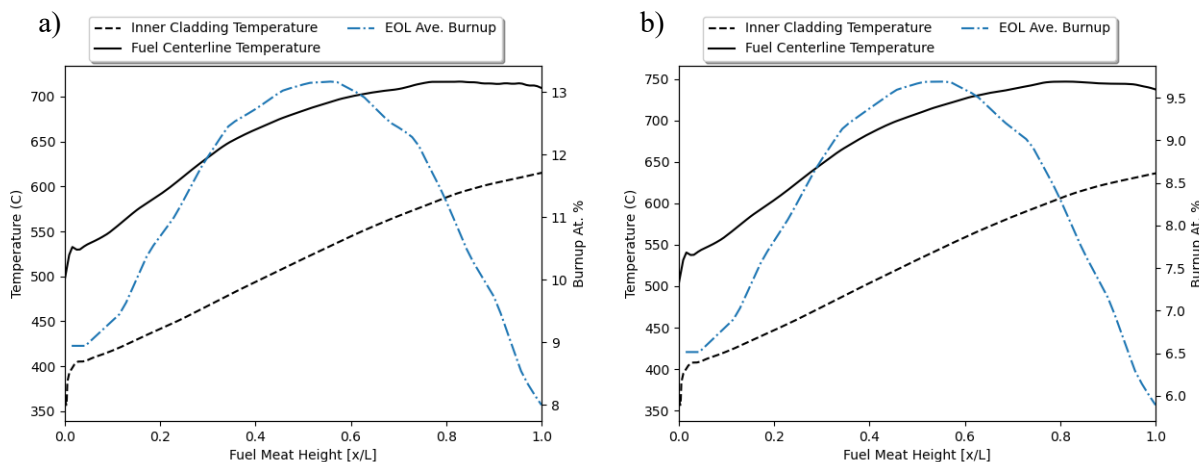


Figure 4: Simulated FCT, ICT, and End of Life Burnup for a) 193045 and b) 195011

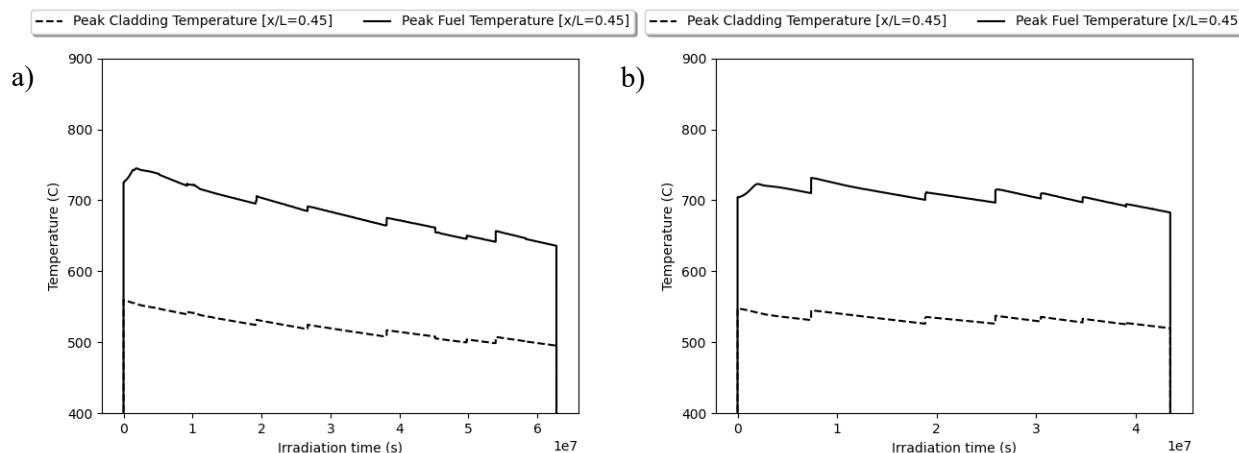


Figure 5: Simulated PFCT and PICT over time for a) 193045 and b) 195011

## 4.2 Profilometry

The profilometry performed on metallic fuel experiments is used as an indication of the strain that the cladding is experiencing due to FCCI and FCMI. Accurately modeling the cladding profile will help in understanding the underlying factors that cause the cladding deformation without relying on PIE which can be destructive. The profilometry of all 169 MFF pins have been simulated. Figure 6 shows the simulated profilometry of pins 193045 and 195011 compared with the experimental results from PIE. The BISON simulation predicts both peaks of the 193045 profilometry, but it overpredicts the displacements in between the peaks. This indicates that plasticity of the fuel and cladding play a more significant role in the deformation of the cladding than is currently predicted by the model. This is further evidenced by the comparison between the simulation and experiment of pin 195011. The peak at the top of the fuel is predicted well, but the lower peak is overpredicted significantly. This indicates that these locations would contain vital information needed to further understand interactions between the fuel and cladding.

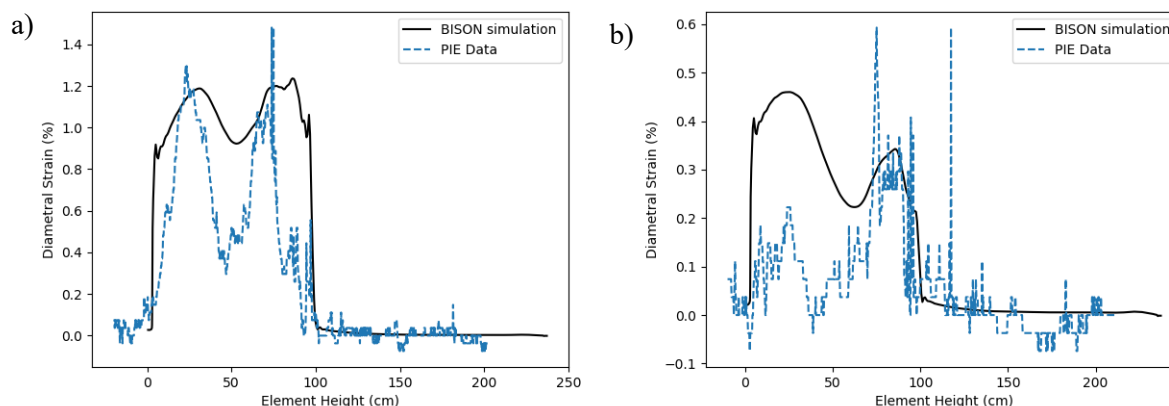


Figure 6: Simulated and Experimental Profilometry Results for a) 193045 and b) 195011



### 4.3 Fission Gas Release and Plenum Pressure

The fission gas released from the metallic U-Zr fuel is an important parameter for understanding the evolution of the plenum behavior. The increase of gas content in the plenum leads to a buildup of pressure in the plenum. Verifying that the plenum remains structurally sound is a primary concern for fuel performance simulations, as failure would lead to the release of fission gases into the atmosphere. The fission gas release can also inform researchers on porosity and burnup behaviors in the fuel. Table 5 compares burnup, plenum pressure, and fission gas release values taken from PIE with simulation results. This shows that while the burnup of both pins is overpredicted compared to experimental results, the plenum pressure and fission gas release are significantly underpredicted. This implies that the interconnection and porosity models are underpredicting the connection of pores to the exterior and therefore are not releasing as much fission gas. This is further demonstrated by the fission gas produced being simulated accurately compared to the experimentally calculated fission gas production results. Further refinement of the `ADSimpleFissionGasViscoplasticityStressUpdate` settings in the BISON fuel performance code will be needed to correct this underprediction.

Table 5: Burnup, Plenum Pressure, and Fission Gas Released Comparison [11]

Pin Number	193045		195011	
	PIE	BISON	PIE	BISON
Peak BU (a/o)	13.8	15.9	10.1	11.7
Avg BU (a/o)	10.85	11.2	7.61	8.26
Fission Gas Produced (Moles)	0.0314	0.0359	0.0233	0.0264
Plenum Pressure (PSI)	322.4	118.4	272.3	109.4
Fission Gas Release (%)	61	29	79	36

### 4.4 Fuel Cladding Chemical Interaction

The FCCI is a key parameter for fuel performance as excessive amounts of FCCI can lead to structural and thermal degradation of the cladding. Accurate predictions of the FCCI layer location and depth will allow for targeted PIE at locations where FCCI development is predicted to occur. Targeted investigations of these regions will have a significant impact on the understanding of the driving mechanisms behind FCCI moving into the future. Table 6 shows the simulated maximum FCCI layer depth compared to PIE results for different axial locations. The comparison shows that the FCCI layer depth model follows the axial temperature prediction seen in Figure 4. Unfortunately, the results for pin 195011 show that there are potentially significant contributions to the FCCI phenomenon that are not being accounted for at the top location of the fuel pin. As more mechanistic models become available, FCCI simulations will need to be reassessed to ensure that this behavior is captured by the simulations.



Table 6: Comparison of Simulated FCCI with PIE [11]

Pin Number	Axial Location (x/L <sub>0</sub> )	Height from BOF (cm)	Measured Max FCCI Depth (μm)	Simulated Max FCCI Depth (μm)
193045	0.03	2.5	0	1.9
	0.24	22.9	0	6.2
	0.49	45.7	0	27.4
	0.74	68.5	76	79.2
	0.98	91.4	152	128.5
195011	0.03	2.5	0	1.6
	0.24	22.9	0	5.3
	0.48	45.7	0	23.9
	0.72	68.6	51	70.9
	0.96	91.4	25	118.3

## 4.5 Zirconium Redistribution

The zirconium redistribution is a diffusion-based phenomenon that can significantly impact the physical integrity, thermophysical properties, and chemical behaviors of the fuel. Accurately simulating the redistribution of zirconium in U-Zr metallic fuel is an important aspect of determining the location of significant FCCI and FCMI within the fuel for further investigation with PIE. The zirconium redistribution has been modeled for all 169 MFF pins. Figure 7 shows the simulated zirconium content at the end of life compared to the metallography for pin 193045. The profile and shape of the simulated zirconium concentration follows the trend of the radial zones seen in the metallography sections. This is encouraging for future simulation work to predict thermophysical property development more accurately in the fuel throughout irradiation.



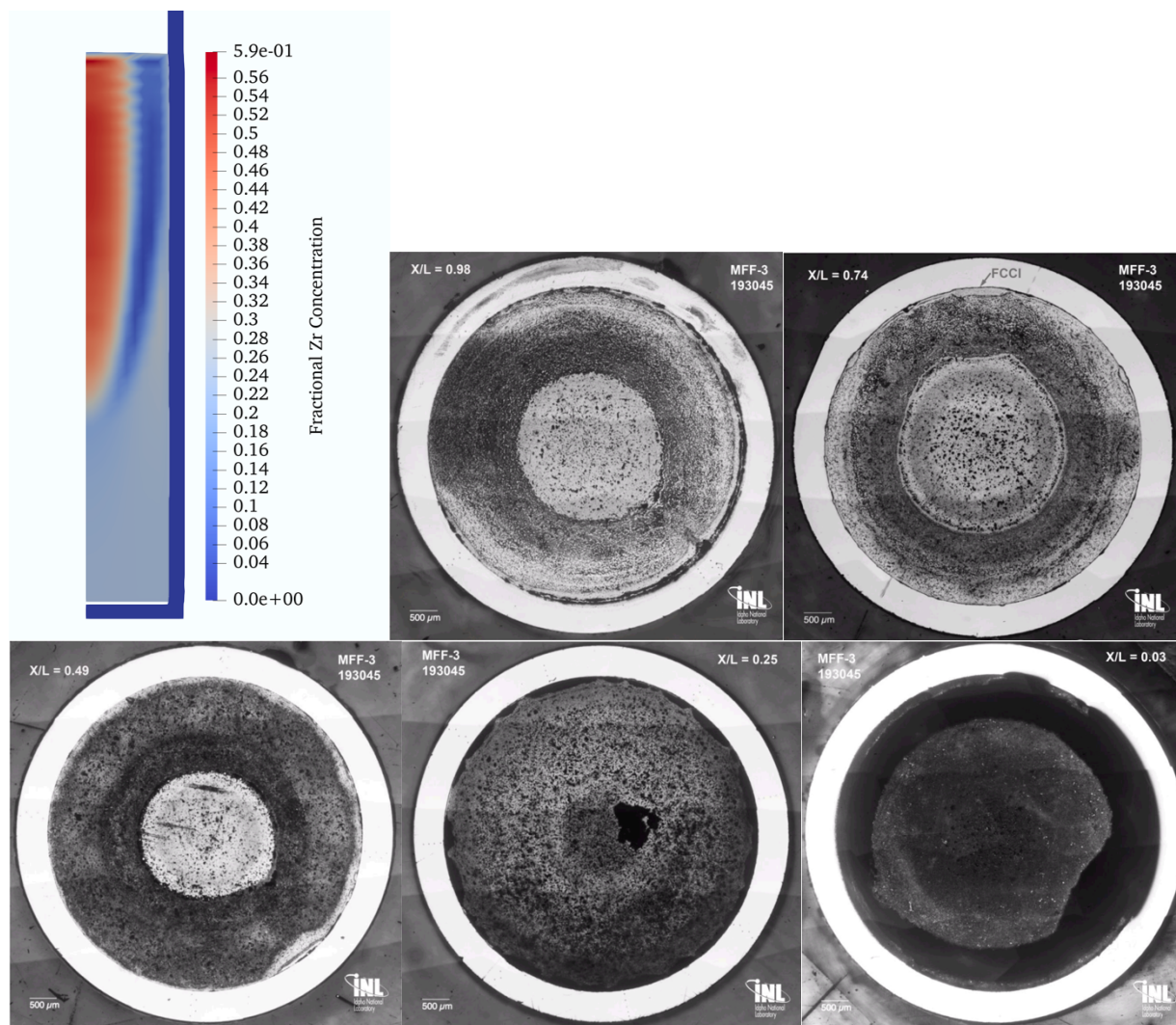


Figure 7: Simulated Fractional Zirconium Concentration Compared to Metallography of 193045 [11]

## 5. Conclusions

This report has addressed the current state of the FFTF MFF experiment fuel performance simulations, and the support offered to PIE with these simulations. Specifically temperature profiles, profilometry, fission gas release, plenum pressure, and zirconium redistribution have been simulated. Metallic U-Zr nuclear fuel alloy has regained interest as a promising candidate fuel for the next generation SFRs. It is integral that modeling efforts be used to direct new efforts in PIE. Simulations can help understand the underlying behaviors leading to PIE observations and indicate regions of interest for new PIE investigation. This simulation directed PIE will allow for the conservative use of the critical and limited resources of legacy metallic fuel experiment materials.



## 6. References

- [1] T. Ogata, Y. S. Kim, A. Yacout, "Metal Fuel Performance Modeling and Simulation," *Comprehensive Nuclear Materials*, 2020, doi: <https://doi.org/10.1016/b978-0-12-803581-8.11676-5>.
- [2] T. Ogata, "3.01 - Metal Fuel," in *Comprehensive Nuclear Materials*, R. J. M. Konings Ed. Oxford: Elsevier, 2012, pp. 1-40.
- [3] G. L. Hofman, L. C. Walters, and T. H. Bauer, "Metallic fast reactor fuels," *Progress in Nuclear Energy*, vol. 31, no. 1, pp. 83-110, 1997/01/01/ 1997, doi: [https://doi.org/10.1016/0149-1970\(96\)00005-4](https://doi.org/10.1016/0149-1970(96)00005-4).
- [4] R. S. F. D. E. Burkes, D.L. Porter, "Metallic fast reactor fuel fabrication for the global nuclear energy partnership," *Journal of Nuclear Materials*, vol. 392, 2009, doi: <https://doi.org/10.1016/j.jnucmat.2009.03.009>.
- [5] W. J. Williams, D. M. Wachs, M. A. Okuniewski, and S. van den Berghe, "Assessment of swelling and constituent redistribution in uranium-zirconium fuel using phenomena identification and ranking tables (PIRT)," *Annals of Nuclear Energy*, vol. 136, p. 107016, 2020/02/01/ 2020, doi: <https://doi.org/10.1016/j.anucene.2019.107016>.
- [6] D. C. C. D.L. Porter, "Fuel Performance Design Basis for the Versatile Test Reactor," *Nuclear Science and Engineering*, 2022, doi: <https://doi.org/10.1080/00295639.2021.2009983>.
- [7] M. T. A. Aitkaliyeva, J. Hirschhorn, J. Powers, I. Greenquist, B. Beeler, "Research Needs for Uranium-Zirconium- Based Metallic Fuels," 2020.
- [8] P. N. N. Laboratory, "Fast Flux Test Facility," 2020.
- [9] D. C. Crawford, D. L. Porter, and S. L. Hayes, "Fuels for sodium-cooled fast reactors: US perspective," *Journal of Nuclear Materials*, vol. 371, no. 1, pp. 202-231, 2007/09/15/ 2007, doi: <https://doi.org/10.1016/j.jnucmat.2007.05.010>.
- [10] R. B. B. A.L. Pitner, "Metal fuel test program in the FFTF," *Journal of Nuclear Materials*, vol. 204, pp. 124-130, 1993, doi: [https://doi.org/10.1016/0022-3115\(93\)90208-G](https://doi.org/10.1016/0022-3115(93)90208-G).
- [11] W. J. Carmack, D. L. Porter, D. G. Cummings, H. M. Chichester, S. L. Hayes, and D. W. Wootan, "Examination of Legacy Metallic Fuel Pins (U-10Zr) Tested in FFTF," Idaho National Laboratory (INL), Idaho Falls, ID (United States), 2020-05-01 2020. [Online]. Available: <https://www.osti.gov/biblio/1617195>  
<https://www.osti.gov/servlets/purl/1617195>
- [12] J. V. N. D.W. Wootan, "IRRADIATION DATA FOR THE MFF-3 AND MFF-5 TESTS IN THE FFTF," 2011, doi: <https://doi.org/20249>.
- [13] Y. S. Kim, S. L. Hayes, G. L. Hofman, and A. M. Yacout, "Modeling of constituent redistribution in U&ndash;Pu&ndash;Zr metallic fuel," *Journal of Nuclear Materials*, vol. 359, no. 1-2, pp. 17-28, December 1, 2006 2006. [Online]. Available: [http://sciserver.lanl.gov:80/cgi-bin/sciserv.pl?collection=journals&journal=00223115&issue=v359i1-2&article=17\\_mocriumf](http://sciserver.lanl.gov:80/cgi-bin/sciserv.pl?collection=journals&journal=00223115&issue=v359i1-2&article=17_mocriumf)
- [14] M. C. Billone, Y. Y. Liu, E. E. Gruber, T. H. Hughes, and J. M. Kramer, "Status of Fuel Element Modeling Codes for Metallic Fuels," in *American Nuclear Society International Conference on Reliable Fuels for Liquid Metal Reactors*, Tuscon Arizona, September 7-11, 1986 1986: ANS.
- [15] H. Savage, "The heat content and specific heat of some metallic fast-reactor fuels containing plutonium," *Journal of Nuclear Materials*, vol. 25, no. 3, pp. 249-259, 1968/03/01/ 1968, doi: [https://doi.org/10.1016/0022-3115\(68\)90168-2](https://doi.org/10.1016/0022-3115(68)90168-2).
- [16] G. L. Hofman *et al.*, "Metallic Fuels Handbook," United States, 2019-04-10 2019. [Online]. Available: <https://www.osti.gov/biblio/1506477>  
<https://www.osti.gov/servlets/purl/1506477>



- [17] D. R. Olander, "Fundamental aspects of nuclear reactor fuel elements," United States, 1976-01-01 1976. [Online]. Available: <https://www.osti.gov/servlets/purl/7343826>
- [18] K. A. G. J.D. Hales, B.W. Spencer, S.R. Novascone, G. Pastore, W. Liu, D.S. Stafford, R.L. Williamson, D.M. Perez, R.J. Gardner, "BISON Users Manual - BISON Release 1.2," 2015.
- [19] L. A. N. Laboratory, "AFCI Materials Handbook, Materials Data for Particle Accelerator Applications, Chapter 18 - Design Properties of HT9 and Russian Ferritic/Martensitic Steels, Rev 6," 2014.
- [20] I. E. P. K.J. GeelHood, "Modeling and Assessment of EBR-II Fuel with the US NRC's Fast Fuel Performance Code," presented at the TopFuel, Prague, 2018.
- [21] L. Leibowitz and R. A. Blomquist, "Thermal conductivity and thermal expansion of stainless steels D9 and HT9," *International Journal of Thermophysics*, vol. 9, no. 5, pp. 873-883, 1988/09/01 1988, doi: 10.1007/BF00503252.
- [22] T. Y. T. Ogata, "Development and validation of ALFUS: an irradiation behavior analysis code for metallic fast reactor fuels,," *Nuclear Technology*, 1999, doi: <https://doi.org/10.13182/NT99-A3018>.
- [23] A. Kayahan, "Modelling of thermo-mechanical and irradiation behavior of metallic and oxide fuels for sodium fast reactors," PhD, Nuclear Science and Engineering, Massachusetts Institute of Technology, Boston MA, 2010-08-30T14:39:56Z, 2009.
- [24] J. B. A. Karahan, "A new code for predicting the thermo-mechanical and irradiation behavior of metallic fuels in sodium fast reactors," *Journal of Nuclear Materials*, 2010.